Grid-Connected Hybrid PV–Wind Microgrid Using ANFIS-Based Control for DC-Link Regulation and dq-PLL Synchronization

1. Jakka Priya Darshini
EEE, GNITS
Hyderabad, India
24251d5403@gnits.ac.in

2. Dr. Ranuva Nageswara Rao
EEE, GNITS
Hyderabad, India
nagesh.ranuva@gnits.ac.in

***Abstract*—Hybrid PV-wind microgrid are strongly nonlinear and high rate of transient disturbance by irradiance and wind speed, which directly impact on the DC-link stability and power quality in the grid. This work includes a Matlab/Simulink version of a grid connected hybrid renewable microgrid that consists of the PV array with perturb and observe (PO) maximum power point tracking (MPPT) and the wind energy conversion system based on a wind turbine-driven permanent magnet synchronous generator (PMSG). To improve regulation for a changing operating condition, small rule bases are used for converter/DC-link control with compact Sugeno-type neuro-fuzzy controllers to achieve nonlinear operations without having to frequently retune the gain. Out of PLL scheduled synchronization and dq-axis management of consistent injection of current the grid integration is implemented. Simulation results under step variations in irradiance and wind speed show a reduction in the deviation of the DC-link voltage, faster settling, and better grid current dynamics than conventional control, thus, showing the improved robustness in hybrid renewable integration.**

***Index Terms*—Hybrid microgrid, PV–wind system, Neuro-fuzzy control, Sugeno FIS, DC-link voltage regulation.**

I. Introduction

Microgrids based on hybrid renewable are deployed to maximize the role of renewable generation and minimize reliance on traditional generation generation but intermittency of sources and nonlinearity of power-electronics seriously impact their operation in practice. In grid connected working, accurate synchronisation is an absolute requirement as phase/frequency tracking errors can happen, which degrade the quality and stability of power. It is the design trade-offs of modern three phase phase-locked loop (PLL) structure and dynamics that are now the key to reliable grid interfacing of converter-based resources, particularly at weak-grid disturbances or at the disturbed grid [1]. Further, a survey on the power point decision of PLL synchronization in grid-connected renewable systems clearly shows that synchronization decisions can have a direct effect on the robustness of the inverter control system during dynamic operating scenarios [2].

On the generation side, the output of photovoltaic (PV) varies rapidly with the irradiance and temperature conditions that there is a need to use maximum power point tracking (MPPT). Traditional MPPT and converter regulators usually have to be retuned (at different operating points) which drives intelligent controllers to be able to capture nonlinear mappings. Adaptive neuro-fuzzy inference system (ANFIS) based approaches have been widely investigated for PV modeling and MPPT because of their capability of dealing with nonlinear characteristics with rule based learning [3]. Under unfavorable conditions such as partial shading, ANFIS-based global MPPT strategies have demonstrated enhanced tracking capability as compared to simpler strategies [4]. Beyond simulation, ANFIS MPPT and reference model control concepts have also been realized on hardware platforms such as FPGA (Field Programmable Gate Array) which proves the practical feasibility for real-time renewable energy conversion [5]. Similarly, advanced control strategies such as sliding mode control for operating hybrid PV and wind-battery microgrids have been reported with respect to improvement in dynamic performance in the event of disturbances, thus adding to the need for solid nonlinear control for hybrid microgrids [6].

Novelty and Contributions: The work is novel in the sense that the article presents a fully pulse to end-to-end implementation of a hybrid PV-wind grid-connected microgrid with focus on compact joint neuro-fuzzy control practical to tune and that is light in computations. The main contributions are:

- Development of a complete MATLAB/Simulink-based hybrid PV–Wind microgrid model incorporating source-side power electronic converters, DC-link coupling, and grid-side inverter interfacing to enable integrated system-level evaluation rather than isolated subsystem analysis.
- Design and implementation of compact rule-base neuro-fuzzy controllers for converter and DC-link voltage regulation, aimed at enhancing transient stability across the entire operating range without repeated gain retuning.
- Implementation of PLL-based grid synchronization and dq-axis current control strategy with two-step static grid injection. Dynamic performance is validated through step-change disturbances in solar irradiance and wind speed to evaluate system stability and robustness.

II. Related Work

Hybrid PV Wyatt microgrids are widely studied as there is no doubt that it is smart to use two complementary sources of renewable energy which increase reliability and thus avoid

having to rely on one single intermittent resource. Many of the works start with the planning and sizing phase in which the intention is to determine the best PV and wind capacities for a given site and load. Hosny et al. present an optimal sizing study for PV-wind microgrid using a real case study demonstrating how the local resource availability and the demand patterns influence the final microgrid configuration and the feasibility results. [7]

After sizing, the next technical requirement is that of grid interfacing through power electronic converters where synchronization and current control give rise to stability and quality of power. Teodorescu, Liserre and Rodriguez present a solid basis of grid converters for PV and wind systems along with inverter structures, synchronization concepts and dq-reference frame current control methods that are widely used for grid connected renewable systems. [8]

To cope with the high nonlinearity and dependence on operating point of renewable conversion, researchers have considered the use of intelligent control, in particular neuro-fuzzy control. Jang introduced the adaptive neuro-fuzzy inference system (ANFIS), providing the framework of the combination of fuzzy inference with adaptive learning to model and control nonlinear systems based on a compact rule-based structure. [9]

In the case of real grid-connected inverters harmonic attenuation is usually accomplished with LCL filters but these filters produce resonance and stability problems so that active damping is required. Ghanem et al. proposed a hybrid active damping solution for LCL-filtered grid-connected converters to suppress the resonance but preserve the dynamic response. [10]

Building on the development of damping, Khan et al. presented an active damping technique based on parallel feedforward compensation of LCL filtered grid connected inverters, with a focus on improvement of stability behaviour and damping effectiveness under grid connected operation. [11]

Parallel to control-focused studies, there are still a number of works that focus on techno-economic planning tools to justify hybrid microgrid deployment. Maity et al. showed the best design of a hybrid microgrid in a university campus using HOMER with Cost-Reliability tradeoffs and configuration assessment before implementation. [12]

At a higher layer of operation, research also looks at managing energy within and optimizing dispatch for the allocation of generation, storage and grid exchange all under multiple objectives. Cui et al. proposed multi-objective optimal dispatch for grid-connected microgrids using artificial hummingbird algorithm which is the general trend in the application of meta-heuristics for supervisory scheduling and operational decision-making. [13]

For LCL filtered converter systems, the damping means of parameter uncertainties must be maintained and grid impedance uncertainties favor under. Said-Romdhane and Mhamis and Mhamis and Han for [14] published robust active damping techniques for LCL-filter based grid connected converters that considered the stability preservation under the practical non-idealities which is really important for reliable grid tied operations.

Microgrids may also operate in the so-called islanded mode or switch between grid-connected and islanded mode, and coordinated strategies may be needed to ensure voltage and power balance. Ding et al studied the control of hybrid AC/DC microgrids in an islanding operational condition which resulted in the importance of coordinated converter control for stable operation in case of disturbances and mode transitions. [15]

Recent hybrid renewable studies continue to use neuro-fuzzy methods for better dynamic response. Bhavani et al., reported GAO–ANFIS based control for a hybrid solar PV and wind power system with a multilevel converter, which gives more reinforcement to the fact that neuro-fuzzy control is effective to deal with nonlinearities and enhance transient control in hybrid renewable systems. [16]

III. Methodology

A. System Configuration

A grid-connected hybrid microgrid is developed in MATLAB/Simulink consisting of a Solar PV subsystem, a Wind energy conversion subsystem, a common DC-link, a battery energy storage (ES) interface, and a three-phase voltage source converter (VSC) connecting the DC bus to the utility grid while supplying an AC load. The common DC-link capacitor buffers short-term power mismatch, and the DC-link voltage V_{dc} is selected as the primary regulated variable since it directly reflects instantaneous power balance between sources, storage, inverter transfer, and load demand. The general Simulink design of the grid-connected PV-wind microgrid is presented in Fig. 1. The subsections below outline the implementation of the PV, wind, DC-link and VSC control.

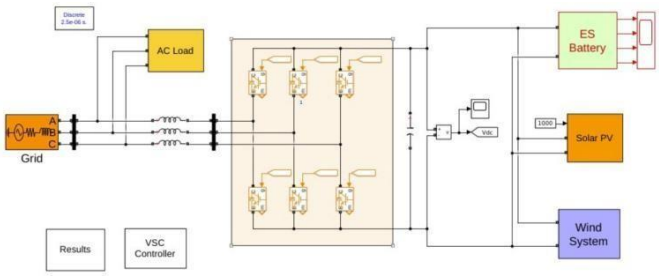

Fig. 1. Simulink block diagram of grid-connected hybrid pv-wind micro grid with common DC and VSC connecting, and battery energy storage.

B. PID vs ANFIS Comparison

PID control is widely used in power-electronic and microgrid applications because of its simple structure and low computational cost. It generates the control signal using the present error, accumulated error, and rate of change of error. However, in a hybrid PV–wind microgrid, irradiance and wind-speed variations continuously shift the operating point, causing the

converter and DC-link dynamics to change. As a result, PID gains tuned for one operating condition may produce higher overshoot, longer settling time, and increased DC-link ripple under sudden renewable disturbances, and repeated retuning may be required to maintain performance.

In contrast, ANFIS (adaptive neuro-fuzzy inference system) implements a nonlinear control law using fuzzy rules with adaptive mapping. ANFIS effectively provides operating-region-dependent control action: it applies stronger correction during large deviations while avoiding overly aggressive action near steady state that can introduce oscillations. Therefore, compact Sugeno-type ANFIS control is more suitable for converter and DC-link regulation in hybrid microgrids, where nonlinearities and parameter variations are significant. This motivates the use of neuro-fuzzy controllers in this work to improve transient damping and reduce oscillations compared to fixed-gain PID regulation.

C. PV Subsystem and MPPT Algorithm

The PV array is connected to the DC bus through a DC–DC conversion stage. Maximum power extraction is achieved using the perturb-and-observe (P&O) method. PV power is computed as

D. Wind Energy Conversion Subsystem

The wind subsystem is modeled using a turbine–generator–converter chain feeding the DC link. Turbine mechanical power is expressed as

$$P_w = \frac{1}{2}\rho A C_p(\lambda, \beta)\, v^3, \tag{1}$$

where ρ is air density, A is the swept area, C_p is the power coefficient, and v is wind speed. The generator output is conditioned using power electronic conversion and delivered to the DC bus. The wind-side control objective is to ensure stable DC-bus contribution during wind-speed disturbances by limiting power oscillations injected into the DC-link.

E. DC-Link Dynamics and Battery Support

The DC link couples PV, wind, ES, and the VSC. The capacitor dynamics relate power imbalance to DC-link voltage deviation:

$$C_{dc} V_{dc} \frac{dV_{dc}}{dt} = P_{pv} + P_w + P_{bat} - P_{inv}, \tag{2}$$

where P_{bat} is battery power (positive during discharge to support the DC bus and negative during charging), and P_{inv} is the power transferred through the inverter to the AC side. Battery ES is used as a buffering element to absorb/supply transient mismatch, thereby reducing peak V_{dc} deviation and improving recovery during sudden renewable or load changes.

F. Grid Synchronization and VSC Control (PLL + dq Current Control)

Grid synchronization is achieved using a three-phase PLL to estimate the grid phase angle ϑ. Using ϑ, three-phase quantities are transformed into the synchronous dq frame. The VSC is controlled using an outer DC-link loop and inner dq current loops.

1) Outer DC-link loop: DC-link error is defined as

$$e_{dc}(t) = V_{dc}^{*} - V_{dc}(t). \tag{3}$$

A PI regulator generates the d-axis current reference:

$$i_d^{*} = K_{p,dc} e_{dc} + K_{i,dc} \int e_{dc}\, dt. \tag{4}$$

The q-axis current reference is set based on reactive power requirement; for unity power factor operation:

$$i_q^{*} = 0. \tag{5}$$

2) Inner current loops: The measured currents (i_d, i_q) are regulated to track (i_d^{*}, i_q^{*}). The controller outputs dq voltage commands (v_d^{*}, v_q^{*}), which are transformed back to abc references and applied to a PWM modulator to generate VSC gating signals. This structure ensures synchronized and balanced grid injection while maintaining DC-link stability.

G. Neuro-Fuzzy (ANFIS) Controller Design

To improve regulation under nonlinear and operating-point-dependent dynamics, Sugeno-type neuro-fuzzy controllers are implemented in the PV path, wind path, and DC-link support loop. The controllers follow an error-based structure using the regulation error and its variation as inputs. The error is defined as

$$e(k) = x^{*}(k) - x(k), \tag{6}$$

and the change in error is computed as

$$\Delta e(k) = e(k) - e(k-1), \tag{7}$$

where x is the controlled variable and x^{*} is the corresponding reference. For DC-link regulation, the controlled variable is V_{dc}, hence

$$e_{dc}(k) = V_{dc}^{*} - V_{dc}(k). \tag{8}$$

All neuro-fuzzy controllers are implemented as Sugeno FIS due to their computational efficiency. Each input is partitioned into three triangular membership functions (`trimf`) representing three operating regions (e.g., Negative/Zero/Positive). A compact rule base is adopted to avoid excessive complexity: the PV-side controller (`ANF.fis`) and wind-side controller (`ANFW.fis`) are two-input/one-output systems with three membership functions per input, resulting in nine rules (3×3), while the DC-link support controller (`ANFDC.fis`) is a single-input/one-output system with three membership functions and three rules.

A generic Sugeno rule is expressed as: If e is A_i and Δe is B_j, then $u = c_{ij}$, where c_{ij} is a constant consequent. The final control output is obtained using weighted averaging:

$$u(k) = \frac{\sum_{r=1}^{N} w_r c_r}{\sum_{r=1}^{N} w_r}, \tag{9}$$

where w_r is the firing strength of the r-th rule. This compact neuro-fuzzy structure provides nonlinear regulation with reduced oscillations and improved transient damping under irradiance and wind-speed disturbances.

TABLE I
SYSTEM PARAMETERS OF THE PROPOSED HYBRID PV–WIND MICROGRID (FROM EV.SLX)

Category	Parameter	Symbol	Value
Grid (3-Phase Source)	Line-line RMS voltage	V_g	230 V
	Grid frequency	f_g	50 Hz
	Source resistance (non-ideal)	R_g	0.8929×10^{-3} Ω
	Source inductance (non-ideal)	L_g	16.58×10^{-9} H
AC Load (3-Phase)	Load connection	–	Y (grounded)
	Nominal load voltage	V_L	230 V
	Active power	P_L	5 kW
	Inductive reactive power	$Q_{L,ind}$	0 var
	Capacitive reactive power	$Q_{L,cap}$	0 var
DC Link	DC-link reference voltage	V_{dc}^*	400 V
	DC-link capacitance	C_{dc}	3500×10^{-6} F (3.5 mF)
	Initial DC-link capacitor voltage	$V_{dc}(0)$	300 V
PV Array	PV module model	–	1Soltech 1STH-215-P
	Module max power	P_m	213.15 W
	Module open-circuit voltage	V_{oc}	36.3 V
	Module short-circuit current	I_{sc}	7.84 A
	Module voltage at MPP	V_{mpp}	29 V
	Module current at MPP	I_{mpp}	7.35 A
	Series modules	N_{ser}	10
	Parallel strings	N_{par}	5
	PV rated power (computed)	$P_{pv,r}$	≈ 10.66 kW
PV Input Conditions	Irradiance (default constant)	G	1000 W/m²
	Temperature (default constant)	T	25°C
Wind Input Condition	Wind speed (default constant)	v	12 m/s
Battery Energy Storage	Nominal voltage	V_{bat}	205 V
	Nominal capacity	C_{bat}	42 Ah
	Initial SOC	SOC_0	65%
	Internal resistance	R_{bat}	0.04881 Ω
	Full voltage	V_{full}	238.6174 V
	Minimum voltage	V_{min}	153.75 V
Control / PWM (DC–DC)	Switching frequency	f_{sw}	5 kHz
	Control/PWM sample time	T_s	10×10^{-6} s

H. Neuro-Fuzzy Control Implementation (Converter Regulation)

To improve dynamic performance under nonlinear operating conditions, Sugeno-type neuro-fuzzy controllers are used within the converter regulation paths. The controllers employ compact rule bases and triangular membership functions, producing a computationally efficient control output through weighted averaging of constant consequents:

$$u = \frac{\sum_{k=1}^{N} w_k c_k}{\sum_{k=1}^{N} w_k}, \tag{10}$$

where w_k is the firing strength of the k-th rule and c_k is its constant consequent. Separate neuro-fuzzy controllers are applied to the PV and wind conversion stages, and an additional compact controller is used for DC-link support regulation, enabling improved damping and reduced oscillations during renewable disturbances. Fig. 3 shows the ANFIS five-layer design that will be employed in the current work, which is fuzzification, rule firing, normalization and consequent evaluation and weighted-sum output generation.

I. Training Method

The ANFIS controllers were created based on a Sugeno-type fuzzy inference systems that has triangular membership functions and small rule base. Parameters tuning is performed in the conventional ANFIS manner where the premise (membership function) and consequent parameters are modified to achieve an optimal output error in normal operating conditions. In MATLAB, training uses a hybrid learning algorithm that uses least-squares estimation (LSE) to estimate consequent

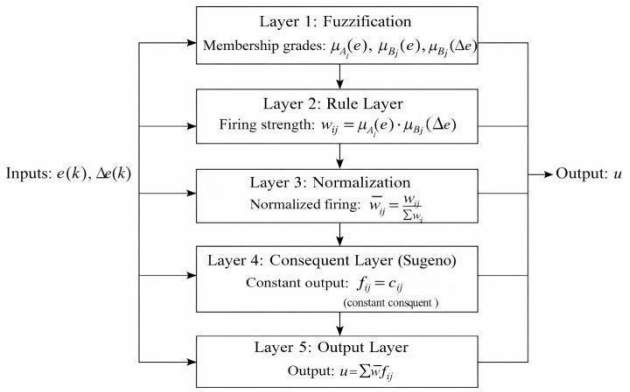

Fig. 2. ANFIS 5-layer Sugeno-type neuro-fuzzy control.

parameters and use gradient descent to estimate premise parameters. The process is repeated through multiple epochs until the error is reduced and the controller is obtained that will provide stable control at different irradiance and load conditions, but with a low computational complexity and better DC-link performance.

1) Why Sugeno Type Was Chosen: Sugeno-type fuzzy inference system was chosen because it is computationally efficient and is suitable in application in real-time control. Sugeno inference makes a crisp output directly, as opposed to Mamdani inference that needs a defuzzification step, as weighted averaging of rule consequents. It gets rid of computational complexity and enhances numerical stability in fast converter control loops. Such efficiency is necessary in a grid-connected hybrid PV-wind microgrid, in which DC-link voltage regulation is used at high sampling rates. Besides, the Sugeno structures can be more conveniently applied to adaptive and hybrid learning-based algorithms and are therefore applicable to ANFIS-based control design.

2) Technical Strength of the Proposed Sugeno-ANFIS Controller.: The proposed Sugeno-ANFIS controller is a type of nonlinear gain scheduler, the operating-region-varying control action which improves damping in DC-link transients, minimizes oscillation yet does not need as many controller gains to be manually adjusted.

J. Validation Scenarios and Metrics

The system is evaluated under three test conditions: (i) irradiance step change, (ii) wind-speed step change, and (iii) combined irradiance and wind disturbance. Performance is assessed using DC-link peak deviation $\Delta V_{dc,\max}$, settling time, and steady ripple, along with PV/wind power responses and grid current stability. These metrics directly quantify the robustness of the hybrid microgrid and the effectiveness of the proposed control strategy under renewable intermittency.

IV. Results And Discussion

The proposed grid connected hybrid PV-wind microgrid was validated in matlab / simulink platform to validate (i) renewable power extraction behaviour, (ii) DC link voltage robustness and (iii) Grid side synchronised current injection. The discussion is organized around three cases of the disturbance that are typically expected in an IEEE microgrid paper: irradiance variation, wind speed variation, and a combination of disturbance representing the worst operating condition.

A. PV Characteristic under the disturbance of irradiance.

For a change in irradiance the operating point of the PV array changes immediately resulting in a corresponding change in V_{pv}, I_{pv}, and P_{pv}. The P&O MPPT drives the PV operating point toward the new maximum power region after the disturbance. The important aspect of the result is not only tracking, but the quality of tracking, the PV-side conversion with the neuro-fuzzy regulation results in a better transient response with less oscillation around the operating point than purely a fixed-step perturbation behavior. This reduction in power hunting is of importance as MPPT oscillations manifest as repetitive disturbances injected in the common DC bus which may generate increased DC link ripple which stresses the inverter stage. Fig. 3 illustrates the dynamics of the power distribution of the system among the grid, PV, wind, battery, and load in response to disturbances in the irradiance.

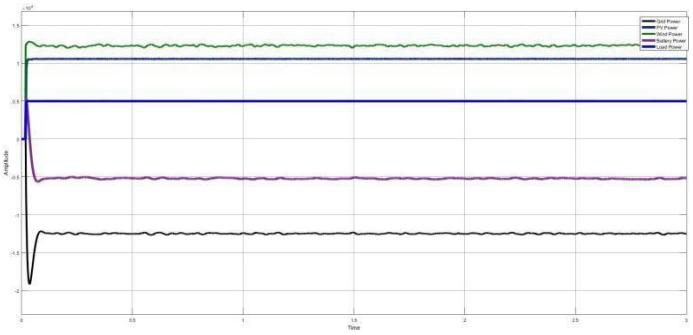

Fig. 3. Dynamics of power generation of Grid Power, PV Power, Wind Power, Battery Power and Load Power at the disturbance of irradiance.

B. Wind Conversion Performance Under Disturbance Of Wind Speed

Stronger nonlinearity is brought about by wind-speed steps because there is aerodynamics of turbines and generator–converter dynamics. With a change in wind speed the electrical output on the wind side takes a transient before reaching a new operating level. The wind-side neuro-fuzzy regulation helps to improve transient damping by reducing overshoot/undershoot and long oscillatory settling is eliminated. As a result, the wind contribution to the dc-link is more controlled which is critical in the case of hybrid schemes where the wind transients lead to the disturbance of the DC link which in turn may destabilize the current analysis on the grid side.

C. DC-Link Voltage Regulation: Primary Indicator of Robustness

The DC-link voltage V_{dc} is the primary stability indicator because it reflects instantaneous power balance among PV, wind, storage, inverter transfer, and load demand. Across the disturbance tests, the system maintains bounded V_{dc} excursions and returns to the reference band without instability. Three consistent improvements are observed:

- **Reduced peak deviation:** the maximum excursion of V_{dc} during disturbance entry is limited, indicating improved disturbance rejection.
- **Faster recovery:** V_{dc} returns to steady regulation more quickly, demonstrating better damping of transient energy mismatch.
- **Lower steady ripple:** after the transient decays, the DC-link voltage exhibits reduced ripple, reflecting smoother power coupling to the inverter.

According to the combined disturbance case i.e. simultaneous changes in irradiance and wind, the highest stress to the DC

link is experienced due to compounded power imbalance. Even in such a worst case, the proposed regulation preserves stable dynamics at the DC link, indicating that the control scheme is robust across the operating regions as opposed to being optimized for a specific operating point.

DC-Link voltage response to variation in irradiance, wind-speed, and a combination of irradiance and wind-speed. ANFIS control has a better regulation compared to the traditional PID control. It is shown in the performance of the DC-link voltage regulation in the event of disturbances, in Fig. 4 where ANFIS control decreases oscillation and stabilizes the voltage quicker than PID control.

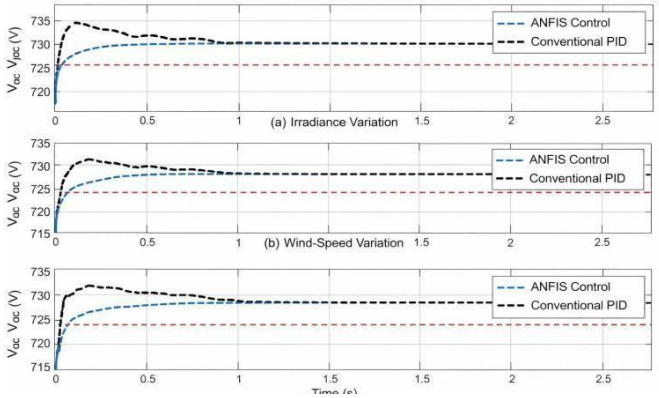

Fig. 4. DC-Link voltage response to variation in irradiance, wind-speed, and a combination of irradiance and wind-speed. ANFIS control has a better regulation compared to the traditional PID control.

D. Role of Battery Energy Storage in Transient Stabilization

The battery ES contributes by absorbing or supplying short-term mismatch power during renewable transients. In the simulations, ES action reduces the depth and duration of DC-link voltage deviation by buffering sudden changes in generation or load. This buffering effect improves the operating conditions for the inverter and avoids abrupt current demand from the grid during renewable fluctuations. In practical terms, ES improves system resilience by preventing DC-link disturbances from propagating strongly to the AC side. According to Fig. 5, the power distribution between the grid, PV, wind, and battery stabilizes during the renewable fluctuations, and the battery aids in the process of flattening the DC-link voltage.

E. Grid-Side Performance:PLL Synchronization and Current Injection.

Grid synchronization is ensured by a three-phase PLL in order to provide the control of dq-axis current for stable injection. During disturbance conditions, the inverter offers the ability of modulating injected current magnitude depending on net available power and keeping phase and with the grid. The three phase remain balanced and stable; it means the grid side control is not destabilized by the fluctuations of source side. Active power is according to the available renewable

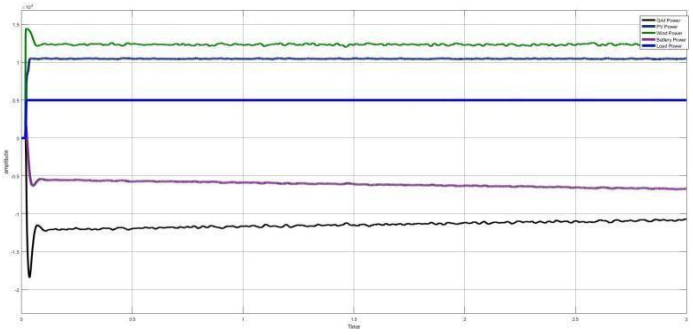

Fig. 5. Power interaction among Grid Power, PV Power, Wind Power, Battery Power, and Load Power in the disturbance of renewable.

generation trend, and reactive power is not far from the set reference (unity power factor operation when $i_q^* = 0$). No loss of synchronization with abnormal shoots in current on transitions; it thus confirms a coordination of operation between regulation via the DC link and grid side current control.

F. Why the Proposed Approach Works Better

Hybrid PV–wind microgrids are nonlinear and they are dependent of the operating point, so the fixed parameter regulation often presents degraded performance with a large variation. The compact Sugeno neuro-fuzzy controllers operate as nonlinear operating-region regulators that use appropriate corrective action at various levels of disturbances and do not cause aggressive oscillation near the steady-state. This helps to reduce the oscillations for source to DC power transfer, therefore it helps the stability of DC link and, therefore results in smoother grid current injection.

G. Overall Outcome

Overall, results of the simulation show that the grid-connected hybrid PV–wind microgrid works well under irradiance and wind speed variables. The proposed neuro-fuzzy-assisted regulation with the aid of DC-link buffering and battery ES enhances the DC-link voltage behavior and ensures synchronized and balanced grid injection under disturbances, which validates the use of the proposed solution for robust hybrid renewable integration.

V. Conclusion

The proposed grid connected hybrid PV-Wind microgrid was implemented and validated successfully in Matlab/Simulink. Simulation results under the irradiance and wind-speed disturbances demonstrate the improvement of the neuro-fuzzy-assisted control for the DC link voltage regulation by decreasing the peak deviation, increasing the recovery time, and reducing the steady-state ripple. Battery energy storage is further used to smooth the transient power imbalance while the PLL-based dq control allows to maintain synchronized and balanced grid current injection. In general, the system shows a stable and robust operation in the case of renewable

intermittent conditions, which justifies the relevance of the suggested control strategy in the integration of a hybrid microgrid.

REFERENCES

[1] S. Golestan, J. M. Guerrero, and J. C. Vasquez, "Three-phase PLLs: A review of recent advances," *IEEE Transactions on Power Electronics*, vol. 32, no. 3, pp. 1894–1907, Mar. 2017, doi: 10.1109/TPEL.2016.2565642.

[2] Z. Ali, N. Christofides, L. Hadjidemetriou, E. Kyriakides, Y. Yang, and F. Blaabjerg, "Three-phase phase-locked loop synchronization algorithms for grid-connected renewable energy systems: A review," *Renewable and Sustainable Energy Reviews*, vol. 90, pp. 434–452, 2018, doi: 10.1016/j.rser.2018.03.086.

[3] R. Kharb, S. L. Shimi, S. Chatterji, and M. F. Ansari, "Modeling of solar PV module and maximum power point tracking using ANFIS," *Renewable and Sustainable Energy Reviews*, vol. 33, pp. 602–612, May 2014, doi: 10.1016/j.rser.2014.02.014.

[4] F. Belhachat and C. Larbes, "Global maximum power point tracking based on ANFIS approach for PV array configurations under partial shading conditions," *Renewable and Sustainable Energy Reviews*, vol. 77, pp. 875–889, Sep. 2017, doi: 10.1016/j.rser.2017.02.056.

[5] A. A. Aldair, A. A. Obed, and A. F. Halihal, "Design and implementation of ANFIS-reference model controller based MPPT using FPGA for photovoltaic system," *Renewable and Sustainable Energy Reviews*, vol. 82, pp. 2202–2217, 2018, doi: 10.1016/j.rser.2017.08.071.

[6] H. Al-Mattarneh *et al.*, "Sliding mode control-based grid connected PV-wind-battery powered microgrid system," in *Proc. 2025 IEEE 5th Int. Conf. on Sustainable Energy and Future Electric Transportation (SEFET)*, Jaipur, India, 2025, pp. 1–7, doi: 10.1109/SEFET65155.2025.11255067.

[7] E. M. Hosny, M. S. Soliman, H. M. A. Mageed, M. M. Samy, and A. Y. Abdelaziz, "Optimal sizing of a microgrid based on PV-wind: A case study of a resort in Matruh Government, Egypt," in *Proc. 2024 25th Int. Middle East Power System Conf. (MEPCON)*, Cairo, Egypt, 2024, pp. 1–7, doi: 10.1109/MEPCON63025.2024.10850320.

[8] R. Teodorescu, M. Liserre, and P. Rodriguez, *Grid Converters for Photovoltaic and Wind Power Systems*. Hoboken, NJ, USA: John Wiley & Sons, 2011, doi: 10.1002/9780470667057.

[9] J.-S. R. Jang, "ANFIS: Adaptive-network-based fuzzy inference system," *IEEE Transactions on Systems, Man, and Cybernetics*, vol. 23, no. 3, pp. 665–685, May–Jun. 1993, doi: 10.1109/21.256541.

[10] A. Ghanem, M. Rashed, M. Elsayes, and I. I. I. Mansy, "Hybrid active damping of LCL-filtered grid connected converter," in *Proc. IEEE Int. Symp. Power Electronics for Smart Grid (SPEC)*, 2016, doi: 10.1109/SPEC.2016.7846193.

[11] D. Khan, K. Zhu, P. Hu, M. Waseem, E. Ahmed, and Z. Lin, "Active damping of LCL-filtered grid-connected inverter based on parallel feed-forward compensation strategy," *Ain Shams Engineering Journal*, vol. 14, p. 101902, Aug. 2022, doi: 10.1016/j.asej.2022.101902.

[12] A. Maity, S. Kumar, P. Pattanayak, and S. Yadav, "Optimal design of hybrid microgrid for a university campus using HOMER software," in *Proc. 2024 10th Int. Conf. on Electrical Energy Systems (ICEES)*, Chennai, India, 2024, pp. 1–6, doi: 10.1109/ICEES61253.2024.10776827.

[13] B. Cui, H. Yang, X. Luo, X. Wang, and X. Li, "Optimal energy dispatch for grid-connected microgrids based on multi-objective artificial hummingbird algorithm," in *Proc. 2024 43rd Chinese Control Conf. (CCC)*, Kunming, China, 2024, pp. 7179–7184, doi: 10.23919/CCC63176.2024.10661537.

[14] M. Sa¨ıd-Romdhane, M. Naouar, I. Slama-Belkhodja, and E. Monmasson, "Robust active damping methods for LCL filter based grid connected converters," *IEEE Transactions on Power Electronics*, vol. 32, no. 9, pp. 6737–6745, Sep. 2017, doi: 10.1109/TPEL.2016.2626290.

[15] G. Ding, F. Gao, S. Zhang, P. C. Loh, and F. Blaabjerg, "Control of hybrid AC/DC microgrid under islanding operational conditions," *Journal of Modern Power Systems and Clean Energy*, vol. 2, no. 3, pp. 223–232, Sep. 2014, doi: 10.1007/s40565-014-0065-z.

[16] N. V. A. Bhavani, A. Singh, and D. Kumar, "Modeling of GAO-ANFIS controller-based hybrid solar photovoltaic and wind power system with seven-level converter," *Energy Storage and Saving*, vol. 3, pp. 259–269, Dec. 2024, doi: 10.1016/j.enss.2024.05.002.